

Chapter 2

Physicochemical and Electrochemical Characterization

Abstract The different experimental procedures used in this study for the synthesis of various electrode materials and their principle involved are discussed in this chapter. In addition, methodology and principles of different techniques used in the physicochemical and electrochemical characterization of the materials are also discussed in this chapter.

2.1 Introduction

Various synthetic procedures such as hydrothermal, single source precursor approach, sonochemical route and room temperature mechanical stirring have been used in this study to prepare the different electrode materials. The details of these synthetic procedures and the principle involved are discussed in detail in Sect. 2.2. This chapter also provides the details of the different structural, morphological and electrochemical characterization techniques used for the investigation of the synthesized electrode materials. Single crystal X-Ray diffraction (SCXRD), Powder X-Ray Diffraction (PXRD), Temperature dependent (in-situ) X-Ray Diffraction, Quantitative Rietveld refinement of the XRD data, Brunauer-Emmett-Teller (BET) surface area, Raman Spectroscopy, Elemental Analysis (EA) and Thermogravimetric Analysis (TGA) have been utilized in this study for the structural characterization. The morphology of the synthesized materials were studied with the help of Scanning Electron Microscopy (SEM) and Transmission Electron Microscopy (TEM). Electrochemical investigation of the electrode materials were carried out using Galvanostatic cycling, Cyclic Voltammetry (CV) and Electrochemical Impedance Spectroscopy (EIS) studies.

2.2 Synthesis of Electrode Materials

In this study, hydrothermal method was used for the synthesis of cathode materials like LiVOPO_4 and $\text{Li}_2(\text{VO})_2(\text{HPO}_4)_2(\text{C}_2\text{O}_4)$. $\text{K}_2(\text{VO})_2(\text{HPO}_4)_2(\text{C}_2\text{O}_4)$ and its rGO composites were synthesized via three different synthetic routes, namely mechanical stirring at room temperature, grinding and sonochemical reaction. Single source precursor approach was employed for the preparation of $\text{Li}_3\text{V}_2(\text{PO}_4)_3$ and $\text{rGO/Sb}_2\text{S}_3$. Fe_3O_4 nanoparticles wrapped by rGO were obtained by a simple precipitation method followed by annealing at high temperature. The details of the important synthetic procedures such as hydrothermal, single source precursor route and sonochemical reaction are described in detail in the following sections.

2.2.1 Hydrothermal Synthesis

The hydrothermal method involves the synthesis of materials under high vapour pressure and usually at higher temperatures than the boiling point of water [1]. The term hydrothermal is of geologic origin as the conditions beneath the earth crust are similar which helps in the synthesis of different chemicals and crystals. In laboratories, the hydrothermal reactions are usually carried out in a Teflon container enclosed in a stainless autoclave. These conditions help in the synthesis of the desired material at a shorter time and at lower temperatures than the corresponding solid state reaction. In addition, nanoparticles of the desired material can also be obtained with definite particle size and a definite morphology by controlling the synthetic conditions. This technique is also useful for growing single crystals of many organic, inorganic and hybrid materials. If an organic solvent such as ethanol, ethylene glycol, etc., is used instead of water, it is termed as solvothermal synthesis. Ionothermal synthesis utilize ionic liquids as solvents in the synthesis.

In this work, phosphate based materials such as $\text{LiVOPO}_4 \cdot 2\text{H}_2\text{O}$, $\text{Li}_2(\text{VO})_2(\text{HPO}_4)_2(\text{C}_2\text{O}_4) \cdot 6\text{H}_2\text{O}$ were prepared using hydrothermal route. An aqueous solution containing LiOH , oxalic acid, phosphoric acid and V_2O_5 was heated in an autoclave at a temperature of 120°C . Single crystals were obtained for $\text{LiVOPO}_4 \cdot 2\text{H}_2\text{O}$ while $\text{Li}_2(\text{VO})_2(\text{HPO}_4)_2(\text{C}_2\text{O}_4) \cdot 6\text{H}_2\text{O}$ was obtained as green powder by evaporation of the solution obtained after the hydrothermal reaction. These hydrated phases were subjected to dehydration to obtain the anhydrous phases for electrochemical characterization as LIB cathodes.

2.2.2 Single Source Precursor Approach

Single Source Precursor (SSP) approach is a synthetic method used to prepare different inorganic materials like metal oxides [2], metal sulphides [3–5], metal selenides [6, 8] etc. The desired product is obtained from a single molecule which is

used as the precursor, by a single-step decomposition. All the elements that are required in the target compound are incorporated in the precursor molecule. Usually, an organometallic compound or a metal complex is used as the precursor. Decomposition of the single source precursor either in solid state or solution phase yields the desired product in a single step through elimination of unwanted organic moieties [9]. The major advantages of the Single Source Precursor method over other synthetic procedures are:

- Precise stoichiometry of active elements in the desired product
- Synthesis of nanomaterials with good crystallinity and low concentration of impurity
- Lower defect concentrations
- Easier preparation of thin films by chemical vapour deposition (CVD)
- The precursors are often stable in air and less toxic which are easy to handle
- Decomposition at low temperatures compared to other synthetic routes
- Synthesis of the desired compound in a short time.

In this study, Sb_2S_3 and $\text{Li}_3\text{V}_2(\text{PO}_4)_3$ were prepared by the Single source precursor route. The anode material, Sb_2S_3 was prepared by solid state decomposition of $\text{Sb}(\text{SCOPh})_3$ in Argon atmosphere at 400 °C. The cathode material, $\text{Li}_3\text{V}_2(\text{PO}_4)_3$ was made from a Metal Organophosphate Open Framework (MOPOF) material, $\text{Li}_2(\text{VO})_2(\text{HPO}_4)(\text{C}_2\text{O}_4) \cdot 6\text{H}_2\text{O}$ by solid-state decomposition in Argon atmosphere at 800 °C.

2.2.3 Sonochemical Reaction

Sonochemical reaction deals with the synthesis of materials using ultrasonic waves. Sonochemistry arises from the formation, growth of bubbles in a liquid and their implosive collapse [10]. The ultrasonic waves help in the enhancement of the rate of a chemical reaction as many as million folds. These waves excites the atomic and molecular modes like vibrational, rotational, and translational modes thus behaving as a catalyst. Furthermore, the solid reactants used in the reaction are broken into smaller pieces due to the energy released by collapse of the bubbles created by cavitation. This increases the surface area of the reactants which helps the reaction to proceed at an increased rate. In this study, $\text{K}_2(\text{VO})_2(\text{HPO}_4)_2(\text{C}_2\text{O}_4)$ was synthesized by sonochemical route using an ultrasonic bath.

2.3 Structural Characterization

2.3.1 Powder X-Ray Diffraction

Powder X-Ray diffraction (PXRD) is a rapid analytical technique primarily used for phase identification and quantification of crystalline solids and is a non-destructive

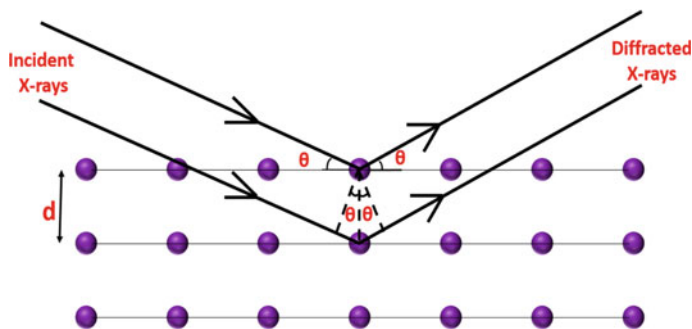


Fig. 2.1 Diffraction of X-rays from crystal lattice

method [11–13]. In addition, it can be used for determination of lattice parameters, space group, crystallite size, degree of crystallinity, residual stress, etc. The analyzed material is ground into a fine powder, homogenized, and the XRD patterns are recorded which determines the average bulk composition of the sample.

The technique relies on the wave-particle duality of X-rays. The wavelength of X-rays are similar to the inter-layer spacing (d -spacing) of the atomic layers in crystalline solids which enables the diffraction of X-rays by crystal lattices of the material under certain circumstances. These diffracted X-rays provide information about the arrangement of atoms in the crystal lattice. Interaction of monochromatic X-rays with a target material results in scattering of these X-rays (Fig. 2.1) which may undergo constructive and destructive interference. The diffraction of X-rays by crystals is determined by the Bragg's law (Eq. 2.1).

$$2d \sin \theta = n\lambda \quad (2.1)$$

where d is the interplanar spacing, θ is the angle between incident X-ray beam and the plane of atoms, λ is the wavelength of the incident X-rays, n is an integer known as order of reflectance. The scattered X-rays result in constructive interference when the Bragg's law is satisfied.

Directions of the possible diffractions be determined by the size and shape of unit cell of the material. Intensities of the diffracted waves of a particular plane are dependent on the arrangement of atoms and their atomic number. However, most solids are not available as single crystals, but contains numerous tiny crystallites which are randomly arranged. When a powder containing many randomly oriented crystallites is placed in an X-ray beam, the beam will meet all possible interatomic planes (Fig. 2.2) and for each set of planes, a certain number of crystals must be oriented at an angle to satisfy the Bragg's law. The peak positions and intensities of the diffracted beams are recorded by the detector. The resultant diffraction pattern is presented in the form of a plot of intensity of diffracted X-rays versus 2θ (degrees). A typical PXRD pattern contains the following information:

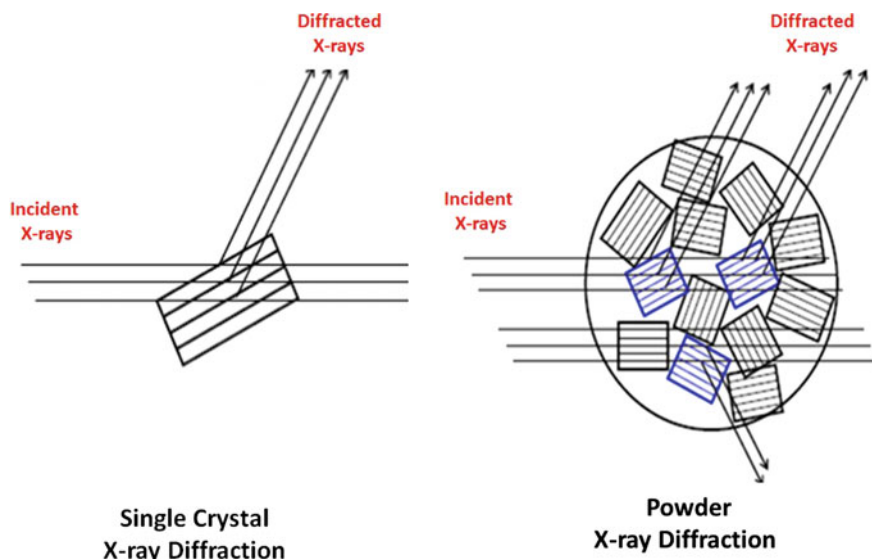


Fig. 2.2 Diffraction of X-rays from a single crystalline sample and a polycrystalline sample

- **Peak Position:** It gives information about the translational symmetry that is the size and shape of the unit cell.
- **Peak Intensity:** It gives information about the electron density inside the unit cell.
- **Peak Shapes and peak widths** give information about deviations from perfect crystal.

The inter-planar spacing, d can be calculated from the Bragg equation ($d = n\lambda/2 \sin \theta$). The International Centre for Diffraction Data (ICDD) offers the database of PXRD patterns of a large number of substances like inorganic, organic, polymer and minerals in the form of Joint Committee on Powder Diffraction Standards (JCPDS) files. As the PXRD pattern is the characteristic of a particular phase, the phase identification of an unknown sample can be primarily identified from the JCPDS files, even if the analyte is a mixture of different phases.

In this study, PXRD patterns of the synthesized compounds were recorded on a Siemens D5005 diffractometer with graphite monochromatised Cu-K α radiation ($\lambda = 1.54056 \text{ \AA}$) or a high resolution Empyrean (Analytical) diffractometer.

2.3.2 *In Situ X-Ray Diffraction*

In-situ X-ray diffraction is a fast and accurate technique to investigate the structure, phases and crystallite sizes of a material during the course of a reaction. Often, the technique is used to record the PXRD patterns at different temperatures, called as

temperature dependent X-ray diffraction. In this technique, the powdered sample was kept in holder and PXRD patterns are recorded at specific intervals of temperature, while the heating or cooling is carried out at a specific rate. In this study, the dehydration of $\text{LiVOPO}_4 \cdot 2\text{H}_2\text{O}$, $\text{Li}_2(\text{VO})_2(\text{HPO}_4)(\text{C}_2\text{O}_4) \cdot 6\text{H}_2\text{O}$ and $\text{K}_2(\text{VO})_2(\text{HPO}_4)(\text{C}_2\text{O}_4) \cdot 4.5\text{H}_2\text{O}$ and were investigated using a Bruker D8 Advance diffractometer (Bruker-AXS GmbH, Karlsruhe, Germany) fitted with Anton Paar high temperature chamber (Model HTK 1200) and low temperature chamber (Model TTK450).

2.3.3 Rietveld Refinement

Rietveld refinement is a basic technique used for the characterization of crystalline materials introduced by Hugo Rietveld. This method is normally used for refinement of neutron and X-ray diffraction pattern of powder samples. The height, width and position of the reflections of a PXRD or neutron diffraction pattern can be used to determine many aspects of the materials structure. In the Rietveld method, a least squares approach is used to refine a theoretical line profile until it matches the experimental pattern. The Rietveld refinement of the XRD patterns were carried out in this study using TOPAS software (version 3.0). The main objective of the Rietveld refinement in this study is to show the phase purity of bulk samples used for the electrochemical studies.

2.3.4 Single Crystal X-Ray Diffraction

Single-crystal X-ray Diffraction is a non-destructive analytical technique which provides detailed information about the structure of crystalline substances. In this technique, a single crystal is mounted on a thin glass fiber and mounted on goniometer head and subjected to X-rays. The diffracted X-rays can be used for the structural solution and refinement. Some of the applications of single-crystal diffraction include:

- Identification, crystal structure solution and refinement of new compounds
- Determination of unit cell, bond-lengths, bond-angles and site-ordering
- Characterization of cation-anion coordination geometry.

In this study, crystal structure of $\text{LiVOPO}_4 \cdot 2\text{H}_2\text{O}$ was determined by single crystal X-ray diffraction. Single crystals suitable for the data collection were selected under an optical microscope, mounted on a glass fiber and the data were collected on a Bruker AXS SMART CCD diffractometer. Graphite-monochromatized Mo-K_α ($\lambda = 0.71073 \text{ \AA}$) radiation was used for data collection. Unit cell dimensions were obtained by least-squares refinements, and the structure was solved by direct methods. The program *SMART* [14] was used for collecting frames of data, indexing

reflections and determining lattice parameters and *SAINT* [14] for integration of intensity of reflections and scaling; *SADABS* [15] was used for empirical absorption correction and *SHELTL* [16] was used for space-group determination, structure solution and least-squares refinements on F^2 .

2.3.5 Elemental Analysis (EA)

Elemental analysis is an important analytical technique used to investigate the composition of a material. The sample is examined for its elemental constituents qualitatively (presence of certain elements) and quantitatively (mass % of different elements). CHNS analysis is the most common application of elemental analysis which provides a means for rapid determination of the elements carbon, hydrogen, nitrogen and sulphur present in organic compounds, polymers and other types of materials. This method relies on the combustion of the sample under investigation at high temperatures ($\sim 1000^\circ\text{C}$) in oxygen-rich environment. In this combustion process, carbon is converted to CO_2 ; hydrogen is converted to H_2O while nitrogen and sulphur are converted to the respective oxides. These combustion products are selectively adsorbed by different traps and the increase in mass of these traps are used to calculate the composition of the sample. In the present study, CHNS elemental analyzer (Elementar Vario MICRO CUBE) was used for the analysis of C, H and S content of the prepared samples.

Quantification of elements other than carbon, hydrogen, nitrogen and sulphur present in the samples can be made by inductively coupled plasma optical emission spectrometry (ICP-OES). This technique uses an inductively coupled plasma which excites the atoms and ions of the different elements present in the sample which emit electromagnetic radiation at certain wavelengths characteristic of that particular element [17]. The intensity of emission determines the concentration of the element within the sample. In this present work, ICP analysis was carried out to determine the quantity of different elements like V, P, Li, K, Fe and Sb. The sample preparation for ICP analysis involves the digestion of samples in certain acids by Milestone microwave laboratory system and the ICP analysis was done using Dual-view Optima 5300 DV ICP-OES system.

2.3.6 Thermogravimetric Analysis

Thermogravimetric analysis (TGA) is an analytical method used to understand the changes in physical and chemical properties of materials [18]. In this technique, a sample is heated at a constant rate and the weight change of the material is monitored as a function of temperature or time. Information on various physical phenomena such as absorption, adsorption, desorption, vaporization and sublimation can be obtained from this method. TGA can also be used to obtain useful

information about chemical phenomena like loss of water or other solvents (dehydration/desolvation), decomposition, oxidation or reduction of the sample. The results are usually represented by a plot of weight of the sample versus temperature and is called a thermogram. The choice of heating rate and the atmosphere such as air, inert gases (He, N₂, Ar, etc.) or vacuum play crucial role on the nature of the plot. The first derivative of the weight loss curve can also be plotted as a function of temperature and is called differential thermogravimetric or DTG curve. This curve can be used to find the precise temperature at which weight loss occurs. In the present work, TGA was used to find out the amount of solvents present in the sample from the corresponding weight losses and the temperature required for preparation of anhydrous phases from hydrated phases. TA Instruments (SDT-2960 Simultaneous DTA-TGA) was used for the analysis with samples weighing ~10 mg in air or N₂ atmosphere.

2.4 Morphological Characterization

2.4.1 *Scanning Electron Microscopy*

Scanning electron microscopy (SEM) is a microscopic technique that uses electron beams instead of light for imaging an object. In SEM, a highly focused beam of high-energy electrons are used to generate a variety of signals at the surface of solid specimens. The signals derived the interaction between the electrons and the sample assist in obtaining information about the sample. Various information such as external morphology, chemical composition, and crystalline structure are obtained from SEM [19].

In this technique, an electron beam is produced by an electron gun at the top of the microscope, which makes a vertical path through the microscope which held within a vacuum. Focusing of the beam towards the sample are possible by electromagnetic fields. Upon the impingement of electron beam on the specimen, it interacts with atoms on the surface which gives rise to different types of radiation. They can provide the basis for surface imaging or analysis of elemental composition of the analyte. Investigation of the specimen mainly involves two types of signals namely, secondary electrons and backscattered electrons. These secondary and backscattered electrons are produced constantly from the surface of the specimen under the electron beam.

When a part of the primary electrons striking the specimen surface are deflected through large angles and re-emitted without energy loss (elastic scattering) from the surface, they are called as backscattered electrons. Since they arise from atomic nucleus interactions, the intensity of the backscattered image depends upon the atomic number of the elements present in specimen. Hence heavy elements are able to backscatter the electrons more strongly and appear brighter in the image while the lighter elements looks less bright. Secondary Electrons are low energy electrons (<50 eV) arising from electron-electron interactions (inelastic events) and are

emitted from the top 5–10 nm zone of excitation area. The amount of secondary electrons depend on the angle of the beam and surface. These secondary electrons are collected by a secondary electron detector (SED) and constitute the basis for the three dimensional imaging of a specimen surface with a scanning electron microscope. The secondary electrons are most valuable as they provide information about the morphology and topography of samples while the backscattered electrons used for illustrating contrasts especially in multiphase samples for phase discrimination.

While there are several other types of signals that are generated by the primary electrons, X-ray signal is typically the only other signal widely used in SEM. This technique called as energy dispersive X-ray spectroscopy (EDS or EDX) is used for the elemental analysis of a sample. X-rays are generated when the primary electrons undergo inelastic collisions with the sample resulting in the excitation of electrons in discrete orbitals. As these excited electrons return to lower energy states, they yield X-rays which exhibit characteristic wavelength and energy patterns of the elements present which leads to its elemental composition.

In the present study, SEM images were recorded with a JEOL JSM-6700F field emission scanning electron microscope (FESEM) operated at 5 kV and 10 μ A. Since electronically-conducting materials are preferable for SEM investigation, samples were coated with a 100 nm thin platinum coating using DC sputtering.

2.4.2 Transmission Electron Microscopy

Transmission electron microscopy (TEM) is a microscopic technique in which a beam of high energy electrons (300 kV) is transmitted through an ultra-thin specimen which interacts with the specimen as it passes through. This interaction produces an image which is enlarged and focused onto an imaging device such as a fluorescent screen or a photographic film. It provides morphological, compositional and crystallographic information of the samples. TEM finds application in metallurgy, materials science, nanotechnology and various fields of biological sciences.

Transmission Electron Microscope produces a high-resolution image from the interaction between the specimen and energetic electrons in a vacuum chamber. The electrons then pass through a series of electromagnetic lenses down the column and make contact with the screen where the electrons are converted to light and form an image of the specimen. By varying the strength of these lenses, magnification of the image can be adjusted. In TEM, the image is acquired as a projection of the entire sample. However, due to electron absorption, only thin specimen sections are used to produce a 2D image on the viewing screen. The brightness of a specific area of the image is proportional to the quantity of electrons that pass through the specimen. Thus, the area of the sample where a large number of electrons can pass through look bright while the dense areas look darker. These provide information on the structure, texture, shape and size of the sample.

2.4.2.1 TEM Sample Preparation

The specimen must be extremely thin for the electrons to pass through, which provide the desired information of the specimen. In this study, the samples containing nanoparticles were dispersed in few mL of ethanol in a closed vial using an ultrasonic bath. The suspended nanoparticles were deposited on to a carbon coated TEM copper grid and dried under vacuum.

2.5 Coin Cell Fabrication

Electrochemical properties of the different electrode materials used in this study were investigated by preparing coin cells (type 2016; 20 mm diameter and 1.6 mm height). The coin cell fabrication involves mainly the following steps:

- Preparation of electrodes of the material under investigation in the form of thin films.
- Assembling the electrode into a coin cell.

The details of these processes are described in the following sections.

2.5.1 Electrode Fabrication

To fabricate the electrode, a slurry was prepared by mixing the active material with super P carbon black and Polyvinylidene difluoride binder (PVDF, Kynar 2801) in a weight ratio of 70:15:15. N-methyl pyrrolidinone (NMP) was used as the solvent in slurry preparation. The slurry was subjected to magnetic stirring for ~ 12 h to ensure homogeneous mixing. Super P carbon is used to provide a continuous carbon network which help the electrons to hop on between the particles to the current collector resulting in enhanced electronic conductivity. The polymer binder PVDF helps in proper adherence of the material on the current collector. The slurry was then coated onto an etched current collector of ~ 10 μm thickness. The choice of current collector depends on the material. Copper foil was used as the current collector for anode materials owing to its excellent electronic conductivity and non-tendency of alloy formation with Li at lower voltages. Aluminium foil is the preferred current collector for cathode materials as copper metal can oxidise at higher voltages. Aluminium forms alloy with lithium at lower voltages and hence it is not a good choice for anode materials.

The coated foil was then dried at 80°C for ~ 12 h for complete removal of the organic solvent, NMP. After proper drying, the composite electrodes of ~ 20 μm thickness were pressed between twin rollers (Soei Singapore Scientific Quartz Co.)

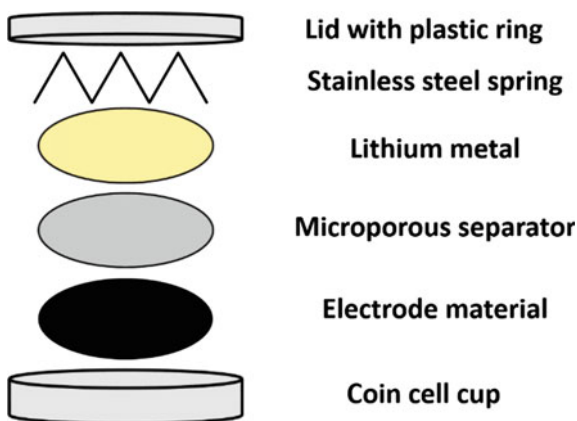
at ~ 2 MPa pressure to ensure good contact between the particles and good adherence of the active material onto the current collector. The electrodes were then cut into circular discs of 16 mm diameter. Selected electrodes were weighed in a high precision balance to calculate the mass of active material in each electrode. The active material content in the electrodes was around 2–5 mg. The electrodes were then dried again in a vacuum oven at 80 °C for 12 h prior to cell fabrication.

2.5.2 Coin Cell Assembly

Coin cells were assembled in an Argon filled glove box (MBraun, Germany) with O_2 and H_2O level maintained below 1 ppm. Li metal (Kyokuto Metal Co., Japan) was mainly used as the counter electrode. Glass microfiber filter (GF/F, Cat No. 1825 055, Whatman Int. Ltd., Maidstone, England) or Celgard (2502) polypropylene microporous membrane was used as the separator. 1 M $LiPF_6$ in ethylene carbonate (EC), dimethyl carbonate (DMC) and diethyl carbonate (DEC) (1:1:1 v/v, Merck) was mainly used as the Li^+ ion conducting electrolyte.

The composite electrode was placed in the bottom cup of coin cell (stainless steel) with the active material facing upwards and the separator was placed above the electrode. Then ~ 50 μL of liquid electrolyte was added to wet the separator, followed by placing the lithium metal and top cap welded with a wave spring (stainless steel). Finally, the coin cells were assembled by crimp sealing in a mechanical hand press. A plastic O-ring was used to prevent the direct contact of cathode and anode which can result in short-circuiting of the cell. It also provides air tight sealing of the cell. A schematic diagram for the coin cell assembly is shown in Fig. 2.3. The fabricated coin cells were aged for 12 h for good percolation of electrolyte into the electrode materials before subjecting to electrochemical studies.

Fig. 2.3 Schematic of coin cell assembly



2.6 Electrochemical Characterization

2.6.1 Galvanostatic Cycling

Galvanostatic cycling or constant current cycling is an important technique for examining the Li storage and cycling behavior of an electrode material. In the current study, the galvanostatic cycling of the cathode materials, LiVOPO_4 , $\text{Li}_2(\text{VO})_2(\text{HPO}_4)_2(\text{C}_2\text{O}_4)$, $\text{rGO}/\text{K}_2(\text{VO})_2(\text{HPO}_4)_2(\text{C}_2\text{O}_4)$ and $\text{Li}_3\text{V}_2(\text{PO}_4)_3$ and the anode materials $\text{rGO}/\text{Sb}_2\text{S}_3$ and $\text{rGO}/\text{Fe}_3\text{O}_4$ were carried out at room temperature (25 °C) using a computer controlled Bitrode multiple battery tester (model SCN, Bitrode, USA). Cycling stability of the materials were investigated by carrying out the lithium cycling for a fairly large number of charge-discharge cycles.

The voltage of an electrochemical cell depends on the state of charge or discharge of the electrode materials of the cell. During galvanostatic cycling, a constant current (I) is applied to the cell and the potential of the cell (V) was monitored as a function of time (t) or state of charge/discharge. The product of the applied current (in ampere) and the time taken (in hours) for complete lithium removal/insertion is the total charge (in mAh) stored by the material and is termed as capacity of the electrode material. The capacity obtained per unit mass of the active material is termed as specific capacity, defined by Eq. 2.2.

$$C = \frac{It}{m} \quad (2.2)$$

where C is the specific capacity in mAh g^{-1} ; I is the current applied in mA; t is the time taken for complete discharge/charge in hours and m is the mass of active material in grams. The theoretical specific capacity of an electrode material is given by the following relation.

$$C_{\text{th}} = \frac{NF1000}{3600M} \quad (2.3)$$

where C_{th} is the theoretical specific capacity in mAh g^{-1} ; F is the Faraday constant (96,496 coulombs per mole) obtained by the product of electronic charge (1.6×10^{-19} C) and Avagadro's number ($6.022 \times 10^{23} \text{ mol}^{-1}$); N is the number of moles of Li^+ ions/electrons involved in the electrochemical reaction per mole of the electrode material and M is the molar mass of the compound in g mol^{-1} . For example, the theoretical capacity of Fe_3O_4 is calculated to be $(96,500 \times 8 \times 1000)/(3600 \times 231.5) = 926 \text{ mAh g}^{-1}$ as 8 mol of Li^+ ions are involved in the lithium storage per mole of Fe_3O_4 . Good reversibility in lithium cycling of an electrode material is often described by the capacity retention over a large number of cycles and is usually represented as a plot of capacity versus cycle number.

2.6.1.1 Rate Capability Studies

For certain applications, faster charging and discharging of a battery is highly desirable. Rate capability studies of an electrode material is a useful method to investigate the lithium storage performance of a material at different current rates. In this study, rate capability of various electrode materials were investigated by carrying out the galvanostatic cycling at different current rates. The following method is adopted to calculate the C rate. If $x \text{ mAh g}^{-1}$ is the theoretical capacity of the material, the applied current densities of 100, 500 and 1000 mA g^{-1} etc., correspond to the C-rates of $100/x$, $500/x$ and $1000/x$ etc. For 1 C current rate, a current density of $x \text{ mA g}^{-1}$ is applied. For different electrode materials investigated in this study, the applied current densities were different, depending on their theoretical capacity and are discussed in individual chapters.

2.6.2 Cyclic Voltammetry

Cyclic voltammetry is an electrochemical technique in which the potential applied to the working electrode is swept at a constant rate and the resulting current is measured as a function of the potential. The current (I) at the working electrode is plotted against the applied voltage (V) to obtain the cyclic voltammogram of the analyte. This technique has found widespread application in understanding the mechanisms of redox reactions, reversibility of a reaction and electron transfer kinetics [20]. The oxidation and reduction potentials of the analyte and the diffusion coefficients of species taking part in the electrochemical reaction can also be found by this method. This method normally uses a three-electrode setup containing a working electrode, a reference electrode and a counter electrode. For a two electrode system such as a coin cell, the counter electrode and the reference electrode are the same.

In cyclic voltammetry, the potential is applied between the reference electrode and the working electrode is ramped between two specified voltage limit at a constant rate in the order of few mV s^{-1} to few V s^{-1} . The voltage is ramped both forward and backward for certain number of cycles and hence the name cyclic voltammetry. As the potential is swept back and forth, a current flows through the electrode that either oxidizes/reduces the analyte and the current (I) between the working electrode and the counter electrode is measured and plotted against the potential. The important parameters in a CV are the anodic and cathodic peak currents ($i_{p,c}$ and $i_{p,a}$) and the corresponding peak potentials $E_{p,c}$ and $E_{p,a}$. By IUPAC convention, the anodic current is positive and the cathodic current is negative. The expression for peak current is given by the Randles-Sevcik expression at 25 °C (Eq. 2.4).

$$I_p = (2.69 \times 10^5) n^{3/2} A C D^{1/2} \nu^{1/2} \quad (2.4)$$

where I_p is the peak current in A, n is the no. of electrons involved in the redox reaction, A is the area of electrode in cm^2 , D is the diffusion coefficient in $\text{cm}^2 \text{s}^{-1}$, C is the bulk concentration of the electroactive species in mol cm^{-3} and ν is the scan rate in V s^{-1} . CVs of the cathode and anode materials prepared in the present study were recorded at room temperature at a scan rate of 0.058 mV s^{-1} employing a computer controlled Mac-pile system (Bio logic, France).

2.6.3 Electrochemical Impedance Spectroscopy (EIS)

EIS is a non-destructive electroanalytical tool used for the evaluation of mechanistic and kinetic information of a wide range of materials like batteries, fuel cells, corrosion inhibitors, etc [21]. In EIS studies of battery systems, the cell is held at equilibrium at a constant voltage and a small amplitude ac-signal is applied. The response of the system to this perturbation from equilibrium is measured in terms of the amplitude and phase of the resultant current. This provides information about the overall impedance of the cell. The frequency of the ac-signal is varied and the impedance of the cell is recorded as a function of frequency. The impedance is represented as a complex quantity z comprising of ‘in phase’ (Z_{re}) and ‘out of phase’ (Z_{im}) impedances. The plots of imaginary versus the real impedance at different frequencies are called Nyquist plots. EIS provides a means to understand the detailed kinetic and mechanistic information to monitor the battery properties under different conditions such as:

- Analysis of state of charge
- Investigation of reaction mechanisms
- Evaluation of electrode kinetics of each electrode
- Change of active surface during operation
- Evaluation of separators
- Passivating film behaviour
- Identification of possible electrode corrosion process.

The total impedance of a cell is the combination of different processes occurring during cycling, namely, diffusion, electron transfer kinetics, charge transfer impedance, bulk impedance, passivating layers, Warburg impedance and intercalation capacitance. The relative contributions of these different processes depends on frequency. The electron transfer kinetics dominates at high to intermediate frequency range (1 MHz–1 kHz). The diffusion process dominates in the low frequency range (1 kHz–3 MHz). Therefore, the EIS measurements were carried over wide frequency range of 180 kHz–0.001 Hz.

In this study, impedance spectroscopy measurements were carried out using Solartron 1260 A impedance analyzer. An ac-signal with amplitude of 5 mV is used to measure the impedance response over the frequency range of 180 kHz–0.001 Hz. The Nyquist plots were examined to determine the individual components constituting the overall impedance using Zview software by fitting an equivalent electrical

circuit to the Nyquist plots. These models (circuits) are designed using combination of constant phase elements (CPE) and resistors in parallel or series to match the observed Nyquist plots.

References

1. K. Byrappa, M. Yoshimura, *Handbook of Hydrothermal Technology* (Elsevier, 2001)
2. S. Daniele, R. Papiernik, L.G. Hubert-Pfalzgraf, S. Jagner, M. Håkansson, *Inorg. Chem.* **34**, 628–632 (1995)
3. J. Sun, W.E. Buhro, *Angew. Chem. Int. Ed.* **47**, 3215–3218 (2008)
4. S.L. Cumberland, K.M. Hanif, A. Javier, G.A. Khitrov, G.F. Strouse, S.M. Woessner, C.S. Yun, *Chem. Mater.* **14**, 1576–1584 (2002)
5. P.S. Nair, T. Radhakrishnan, N. Revaprasadu, G. Kolawole, P. O'Brien, *J. Mater. Chem.* **12**, 2722–2725 (2002)
6. J.J. Vittal, T.N. Meng, *Acc. Chem. Res.* **39**, 869–877 (2006)
7. M.A. Malik, P. O'Brien, N. Revaprasadu, *Adv. Mater.* **11**, 1441–1444 (1999)
8. S.L. Castro, S.G. Bailey, R.P. Raffaele, K.K. Banger, A.F. Hepp, *Chem. Mater.* **15**, 3142–3147 (2003)
9. N.O. Boadi, M.A. Malik, P. O'Brien, J.A.M. Awudza, *Dalton Trans.* **41**, 10497–10506 (2012)
10. K.S. Suslick, *Sci. Am.* **260**, 80–86 (1989)
11. L.V. Azaroff, M.J. Buerger, *The Powder Method in X-Ray Crystallography* (McGraw Hill, New York, 1958)
12. H. Lipson, H. Steeple, *Interpretation of X-ray Powder Diffraction Patterns* (Macmillan-London, St Martin's Press-New York, 1970)
13. B.D. Cullity, S.R. Stock, *Elements of X-ray Diffraction*, 3rd edn. (Prentice Hall, New York, 2001)
14. *SMART and SAINT Software Reference Manuals Version 5.0, 2000* (Bruker Analytical X-ray Systems Inc., Madison, WI)
15. G.M. Sheldrick, *SADABS, A Software for Empirical Absorptions Correction, Version 2.03, 2001* (University of Göttingen, Göttingen, Germany)
16. *SHELXTL Reference Manual, Version 6.1, 2000* (Bruker Analytical X-ray Systems Inc., Madison, WI)
17. J.I. Goldstein, D.E. Newbury, P. Echlin, D.C. Joy, C.E. Lyman, E. Lifshin, L. Sawyer, J.R. Michael, *Scanning Electron Microscopy and X-Ray Microanalysis*, 3rd edn. (Kluwer Academic, New York, 1994)
18. P. Gabbott, *Principles and Applications Of Thermal Analysis*, 1st edn. (Blackwell, Ames, Iowa, 2008)
19. J. Nolte, *ICP Emission Spectrometry: a Practical Guide* (Wiley-VCH, Weinheim, 2003)
20. D.K. Gosser, *Cyclic Voltammetry: Simulation and Analysis of Reaction Mechanism* (Wiley-VCH, NY, 1993)
21. M.E. Orazem, Bernard Tribollet, *Electrochemical Impedance Spectroscopy* (John Wiley & Sons Inc., New Jersey, 2008)

Phosphate Based Cathodes and Reduced Graphene
Oxide Composite Anodes for Energy Storage
Applications

Hameed, A.S.

2016, XII, 148 p. 86 illus., 73 illus. in color., Hardcover

ISBN: 978-981-10-2301-9